Supplemental material and methods

Mice investigation

Study design, power calculation, blinding of investigators and randomization of mouse samples

The primary endpoint in the mouse studies was to record the effect of *huRANKL* over expression on muscle function (handgrip and running activity) and on glucose levels in response to glucose tolerance test for the *Pparb*$^{-/-}$ mice. Our power analysis suggested that when using 8 mice per group, we would have 80% power to detect a biological significant effect with a 1.6 SD change in glucose levels, and therefore we aimed to use eight mice per group in the different mouse studies. All in vivo experiments and subsequent assessments of the outcomes from these experiments were done in total blinding of the investigators. No experiments requiring randomization of sample groups were performed. All animals of the required genotype were included in the analysis, except for the clamp and labmaster investigation where 2 animals were randomly exclude to have 6 animals per groups.

Generation and genotyping of RANKL transgenic mice and Pparb$^{-/-}$

For the generation of *HuRANKL-Tg+* transgenic mice, a Not I fragment of 200kb containing the *huRankl* gene was isolated from a human genomic BAC clone (RP11-86N24, ImaGenes GmbH) with pulse field gel electrophoresis. The excised band was subsequently run in 4% low melting agarose gel and isolated with β-agarase (New England Biolabs, Paradiesrain, Switzerland) digestion. After dialysis in microinjection buffer, the transgene was microinjected into the pronuclei of fertilized (C57BL/6J x CBA/J)F2 oocytes, as described elsewhere.(1) To identify transgenic founder mice by Southern blot, DNA was isolated from tail biopsies, digested with BamHI, and hybridized with the microinjected fragment. Founder transgenic mice were bred with C57BL/6J mice to establish the various transgenic lines.

HuRANKL-Tg+ progeny were genotyped by PCR (5'TCTTCAACTAATGGTGTACG; 5'TCTACAAGGTCAAGAGCATG). Pr Douni from the Sciences Research Center "Alexander Fleming" Athens, has kindly provided mice.

PPARb$^{-/-}$ mice were generated from a mixed background (Sv129/C57BL/6) and kindly provided by Pr Desvergne from the Genopode Lausanne and have been previously described (2).

Mice were housed five per cage, maintained under standard non barrier conditions and had access to water and standard pellet ad libitum. Mice were maintained on a 12-h light/dark cycle at an ambient temperature of 22-25ºC. All the experience was performed on female and male mice. To measure dynamic indices of bone formation, mice were injected with calcein 9 and 2 days before euthanasia. The animals were killed and blood was collected for serum measurements. Lumbar spine, tibia and femurs were excised for micro-computed tomography (µCT) analysis, histomorphometry, immuhistochemistry, qRTPCR and biomechanical analysis. Gastrocnemius and soleus was for histology and qRTPCR. Animal procedures were approved by the University Of Geneva School Of Medicine Ethical Committee and the State of Geneva Veterinarian Office.

Transgenic copy number

Copy number of the transgene was determined by quantitative real-time PCR (qPCR) using tail DNA from the *HuRANKL-Tg+* mice (Tg5519 lines) and wild-type (*WT*) littermates. qPCR was performed using SsoFast EVA Green Supermix on a Rotor-Gene 6000 RT-PCR machine (Bio-Rad, Corbett Life Science, Cressier, Switzerland). A common pair of primers complementary to both human and mouse *Rankl* gene sequences was used to amplify both genes (5'ACCTGTACGCCAACATTTGC; 5'CTTGGGATTTTGATGCTGGT). For each sample, the Ct value of RANKL was normalized against the mouse HuR gene

(5'AGGACACAGCTTGGGCTACG; 5'CGTTCAGTGTGCTGATTGCT) and the values of both *Rankl* and HuR genes were extrapolated from their respective standard curves.

Challenge mice

Adult phenotype of *HuRANKL-Tg+*

From 4 months of age, female and male *HuRANKL-Tg+* and *WT* mice were characterized (*n* = 8 per group).

HuRANKL-Tg+ mice treated by OPG-Fc and Denosumab

At 4 months of age, female *HuRANKL-Tg+* and *WT* mice received saline (vehicle, Veh), Denosumab (Dmab, 10mg/kg/week) or osteoprotegerin (OPG-Fc, 4mg/kg/week) for 4 weeks. Food consumption was recorded weekly in order to determine if mice eat normally. Denosumab and OPG-Fc were kindly provided by Amgen, Thousand Oaks, USA.

Pparb$^{-/-}$ mice treated by OPG-Fc

At 4 months of age, female *Pparb*$^{-/-}$ mice received saline (vehicle, Veh) or osteoprotegerin (OPG-Fc, 4mg/kg/week) for 4 weeks.

In vivo metabolic phenotyping, Echo MRI

Energy expenditure and the respiratory exchange ratio were determined by indirect calorimetry: locomotor activity was recorded by an infrared frame, and food and fluide intake were measured by highly sensitive feeding and drinking sensors. These parameters were measured in mice housed individually in Labmaster metabolic cages (TSE, Bad Hombourg, Germany) after 5 days of adaptation prior to recording. Such measurements were performed 1 week before the sacrifice. An Echo MRI-700 quantitative nuclear magnetic resonance analyser (Echo medical systems, Houston, TX, USA) was used to measure total lean and fat mass in the HF experiment.

Handgrip test

In vivo hindlimb grip strength was measured using automated grip strength (Bioseb, In Vivo Research Instruments, Vitrolles, France) as previously described (3). Each mouse was tested 5 times with a 40s break between tests. The average peak tension and the best attempts were used as a gauge of muscle strength.

Locomotor activity

Animals were acclimatized to the treadmill (Trottsouris, Ficap, Bray sur seine, France) with a habituation protocol the day preceding the running test. For the evaluation of aerobic maximum speed, exercise workloads are selected to gradually progress in increments from moderate to maximal intensity as previously described (2). The exercise begin with 5 min of exercise at a speed of 8m/min, speed is after increased of 2m/min every 2 minutes. Mice are considered exhausted when they touch 5 times the back of the treadmill, the maximal speed is presented as the aerobic maximum speed. This parameter has been proved a reliable method to prescribe and monitor exercise training (4).

Body temperature measurement

Body temperature was evaluated on 2D images acquired with infrared camera FLIR E60 (FLIR, Täby, Sweden) from 40cm distance perpendicular to the region of interest (eye, dorsal or ventral region). The images were analysed by FLIR Tools software as previously described (5).

Glucose and insulin tolerance tests (GTT and ITT)

After 6h starvation, mice were administered IP with glucose (1.5g/kg) or insulin (0.5U/kg) and glycaemia was measured from tail blood at before the injection, 15, 30, 60, 90 and 120 min after the injection (6).

Collection of serum

Blood from all mice was obtained at baseline and just before euthanasia. After centrifugation, serum was removed and stored at -80°C until analysis. Serum osteocalcin (SBA Sciences, Turku, Finland, and Biomedical Technologies Inc., Stoughton, MA, USA) and myostatin from USBC (United States Biological, MA, USA) were measured by ELISA assay according to manufacturer's instructions.

In vivo measurement of muscle volume and fat infiltration

Micro-computed tomography (VivaCT40, Scanco Medical AG, Basserdorf, Switzerland) was used to assess muscle volume and fat infiltration at the proximal tibia as previously described (7). Briefly, the animals were scanned under gas anesthesia following a standard protocol for bone microstructure measurement. The tibia was pulled to full extension of the stifle joint and the ankle was fixated in a position of approx. 90° flexion. The scanned region was 2.2 mm in length, starting 1m off the growth plate with ø21 mm field of view. The scanner was operated at 55 kV tension, 145 µA current, 200 ms integration time and 1000 projections/180°. Scanning time was 20 min, and total anesthesia duration was 25 min per scan. Each scan consisted of 210 slices reconstructed across an image matrix size of 2048 x 2048 voxels, with an isotropic voxel size of 10.5 µm. Muscle and fat are then segmented from the median image (μ=0.52 cm^{-1} for muscle and 0.01 cm^{-1} for fat (equivalent to -94 and -985 HU respectively)) and quantify in order to have their respective volume.

Ex vivo measurement of bone microarchitecture

Micro-computed tomography (μCT UCT40, Scanco Medical AG, Basserdorf Switzerland) was used to assess trabecular bone volume fraction and microarchitecture in the in the excised 5^{th} lumbar spine body, proximal tibia and distal femur, and cortical bone geometry at the midshaft femoral and tibial diaphysis as previously described (7). Briefly, trabecular and cortical bone regions were evaluated using isotropic 12 μm voxels. For the vertebral trabecular region, we evaluated 250 transverse CT slices between the cranial and caudal end plates, excluding 100 μm near each endplate. For the femoral and tibial trabecular region, to eliminate the primary spongiosa, we analyzed one hundred slices from the 50 slices under the distal growth plate. Femoral cortical geometry was assessed using 50 continuous CT slides (600 μm) located at the femoral midshaft. Morphometric variables were computed from binarized images using direct, three-dimensional techniques that do not rely on prior assumptions about the underlying structure (8). For the trabecular bone regions, we assessed the bone volume fraction (BV/TV, %), Trabecular Thickness (Tb.Th, μm), Trabecular Number (Tb.N, mm^{-1}) and trabecular connectivity density (Tb Conn Density, mm^{-3}). For cortical bone at the femoral and tibial midshaft, we measured the Cortical Tissue Volume (Ct.TV, mm^3), Bone Volume (Ct.BV, mm^3), the Marrow Volume (BMaV, mm^3) and the average Cortical Thickness (Ct.Th, μm).

RNA extraction and Quantitative PCR

Bone, Soleus, gastrocnemius. The whole tibia was immediately excised and bone marrow was flushed before to be frozen liquid nitrogen. Tissu was than pulverized to a fine powder in peqGold Trifast (peQLab Biotechnologie GmbH) using FastPrep System tube and appartus (QBiogene, Illkirch, France) in order to achieve quantitative RNA extraction. We used a lysis time and speed respectively of 14sec and 5 units, as recommended by the maker. Total RNA

extraction and quantitative PCR were performed as previously described (9). The following pre-designed TaqMan® gene expression assays were used for the quantitative RT-PCR (References, *Gapdh*: Mm00437762_m1, *Ranklmouse*: Mm00441908_m1, *Ranklhuman*: Mm012883606_m1, *Pparβ*: Mm01305433_m1, *Pparα*: Mm00627559_m1, *Pparg c1* : Mm01208835_m1, *Lpl*: Mm00434764_m1, *Fas:* Mm01204974-m1, *Fabp4*: Mm00445878_m1, *Glut1*: Mm00600697_m1, *Glut4*: Mm00436615_m1, *Myh1*: Mm01332489_m1, *Myh2*: Mm01332564_m1, *Mstn*: Mm01254559_m1, *Ptp-RG*: , Casp3: Mm01195085_m1, *Bcl2*: Mm00437783_m1, *Fos*: Mm00487425_m1, *Jun*: Mm00495062_m1, *Nfat*: Mn00479445_m1, *Syk*: Mm01333032_m1, *Cid*: Mm00617672_m1, *Tnfα*: Mm99999068_m1, *Ccl5*: , Fgf21: Mm00840165_m1, *Agrin* : Mm01545840, Applied Biosystems, Rotkreuz, Switzerland) consisting of two unlabeled primers and a FAM™ dye-labeled TaqMan® MGB probe, and the correspondent buffer TaqMan® Universal PCR Master Mix (Applied Biosystems, Rotkreuz, Switzerland). Relative quantities (RQ) were calculated with the formula RQ = E-Ct using an efficiency (E) of 2 by default. The mean quantity was calculated from triplicates for each sample and this quantity was normalized to the similarly measured mean quantity of the GAPDH normalization gene. Finally, normalized quantities were averaged for 3 to 4 animals and represented as mean ± SEM.

Immunohistochemistry on C2C12

Pr Foti, Dpt of metabolism & cell physiology, University of Geneva, kindly provided C2C12 myoblasts. C2C12 were cultured in growth medium (DMEM, 4.5 g/L glucose, 1% penicillin-streptomycin) supplemented with 10% FBS. Differentiation into myotubes was initiated by replacing growth medium by a differentiation medium (DMEM, 4.5 g/L glucose, 1% penicillin-streptomycin supplemented with 2% Horse serum) when cells reached 80% confluence as previously described (10). To assess immunocytochemistry of RANK and

RANKL (respectively AF692 and AF462, R&D, Abingdon, UK), cells were fixed, treated with 1% bovine serum albumin, incubated with a goat anti-RANK, or a goat anti-RANKL at a final concentration 1:6000 and incubated at 37 °C for 4h. We than performed the same step than previously described (11). Digital images were obtained using an upright microscope with a camera AxioCam fluo MRc5 controlled by Axiovision AC software (Carl Zeiss MicroImaging GmbH, Germany).

Bone Histomorphometry

To measure dynamic indices of bone formation, mice received subcutaneous injections of calcein (10mg/kg, Sigma, Buchs, Switzerland) 9 and 2 days before euthanasia. Femur were embedded in methyl-methacrylate (Merck, Schaffhausen, Switzerland), and 20-µm-thick transversal sections of the midshaft were cut with a saw (FinOcut, Metkon, Instruments LTD) than sanded to 10-µm-thick and mounted unstained for evaluation of fluorescence. Five-µm thick sagital sections were cut with a Leica Corp. Polycut E microtome (Leica Corp. Microsystems AG, Glattburg, Switzerland) and stained with modified Goldner's trichrome, and histomorphometric measurements were performed on the secondary spongiosa of the proximal tibia metaphysis and on the endocortical and periosteal bone surfaces in the middle of the tibia, using a Leica Corp. Q image analyser at 40X magnification. All parameters were calculated and expressed according to standard formulas and nomenclatures (12): mineral apposition rate (MAR, µm/day), single labeled surface (sLS/BS, %), and double-labeled surface (dLS/BS, %). Mineralizing surface per bone surface (MS/BS, %) was calculated by adding dLS/BS and one-half sLS/BS. Bone formation rate (BFR/BS, $\mu m^3/\mu m^2$/day) was calculated as the product of MS/BS and MAR.

Histological analyses of the muscle

Soleus and gastrocnemius were collected and immediately frozen in methylbutane, then kept at -80 prior to sectioning and staining. 8um sections were cut and mounted on poly-L-Lysine coated slides. Sections were then air-dried, fixed with formalin, and stained with haematoxylin eosin or succinate dehydrogenase as previously described (5). Quantification of number and area of type 1/2 fibers was performed with Bioquant soft (Bioquant Image Analysis Software, Nashville, TN, USA). Qualitatively we also confirm the distribution of type I and II fibers by using specific monoclonal antibodies BA-D5 for type I fibers (secondary Ab: texas red M32017) and SC-71 for type II (secondary Ab: Alexi fluo 488, A21042) provided by Developmental Studies Hybridoma Bank (University of Iowa, Iowa city, Iowa, USA) as previously described (13).

Immunohistochemistry analyses of insulin expression in pancreas

Pancreas was fixed in 4% paraformaldehyde and embedded in paraffin. Four consecutives sections every 125um at 6 different levels were cut. Haematoxylin eosin for islet morphological investigations and insulin staining were performed as previously described (6).

Western blot analysis

Homogenized cells/tissues were lysed in ice-cold RIPA buffer. Lysates were then centrifuged at 6000g for 30 minutes. Lysate supernatants were diluted with equal volumes of twofold concentrated reducing sample buffer containing 125mM Tris buffer (pH6.8), 4% SDS, 20% glycerol, 0.05% bromophenol blue, and 200mM dithiothreitol. Those mixtures were then heated at 70°C for 30 minutes and subjected to gel electrophoresis on 6% to 15% gels. Proteins were electro-transferred to Immobilon P membranes and immunoblotted with specific primary antibodies: Pparγ, CD-36, Actin, SMAD 1/5/8, AKT ser473. Detection was performed using peroxidase-coupled secondary antibody, enhanced chemiluminescence

reaction, and visualization by autoradiography (Amersham International, Little Chalfont, UK). Quantifications were performed using Image J software.

Multiplex assays for measuring inflammatory protein levels

Prior to running the multiplex, extracted soleus and gastrocnemius protein were first sonicated in RIPA buffer and allowed to sit on ice for 30 min. Following 30 min incubation samples were then centrifuged at 13,300 rpm for 15 min at 4 °C and supernatant was taken. BCA Protein Assay Kit was then run to insure equal amount of protein was loaded into multiplex. In supernatant, IL-1α, IL1-β, IL-15, IL-6, mCSF, INFγ, IL-10, Rantes, IL-17α and TNFα levels were determined in duplicate using the Bio-Plex Cytokine Assay (Bio-Rad, Hercules, CA). The Bio-Plex Cytokine assay was read on a Bio-Plex MAGPIX Multiplex Reader and analyzed using the Bio-Plex Manager MP software (Bio-Rad, Corbett Life Science, Cressier, Switzerland).

Humans investigation in post-menopausal women

Subjects

GERICO (Geneva Retirees Cohort http://www.isrctn.com/ ISRCTN11865958) is a prospective ongoing cohort study designed to identify predictive factors of fracture risk in recently retired workers from the Geneva area. Healthy community-dwelling postmenopausal women (n=757) were recruited at the age of 63-67 between 2008 and 2011 by advertisement in the local press, the Geneva University Hospitals, or local large companies at time of retirement. Excluded and included criteria of this cohort have been previously reported in details by Bonnet et al. (14). Subjects were excluded if they had major comorbidities, particularly those with a history of cancer treated in the past 5 years, chronic renal failure, liver or lung disease, corticosteroid therapy, primary hyperparathyroidism, Paget disease of

bone, malabsorption, or any neurological or musculoskeletal condition affecting bone health. The present analysis was conducted in 18 post-menopausal women treated for osteoporosis with Dmab. We evaluated bone density by Dual-energy X-ray absorptiometry using a Hologic QDR Discovery instrument, glucose homeostasis by the evaluation of an index of insulin resistance (Homeostasis Model Assessment of insulin resistance : HOMA) and muscle function by handgrip at baseline and after 3 years as previously performed (15, 16). They were matched to 55 controls and 20 patients treated by bisphosphonate for age, BMI, BMD and fracture. Bisphosphonate group include 12 patients with Zoledronate (5mg/100ml) and 8 patients with alendronate (70mg). The study protocol received the approval from the Geneva University Hospitals' Ethics Committee, and all participants provided written informed consent.

Bone mineral densitometry

Areal BMD at various skeletal sites (lumbar spine, total hip and femoral neck) were determined by Dual-energy X-ray absorptiometry using a Hologic QDR Discovery instrument located in a mobile truck (Hologic Medicor Suisse GmbH, Cham, Switzerland). The coefficient variation of repeated measurements varied between 1.0% and 1.6% for BMD (15, 16) .

Muscle function

Grip strength (kg) was measured to the nearest 0.1 kg using a Jamar® Plus+ Digital hand dynamometer (Sammons Preston, Inc., Bolingbrook, IL, USA). Participants were allowed to perform one test trial, followed by three alternative trials for each hand, and the best measurement was taken for analyses.

Homeostasis Model Assessment of insulin resistance

Blood samples were all taken in the morning, after an overnight fast. HOMA-IR was calculated as [fasting glucose (mmol/L) x fasting insulin (mU/L)] / 22.5 (17). Glucose and insulin were measured on a Cobas-6000 instrument using Elecsys reagents (Roche diagnostics, Roche diagnostics, Switzerland) (18).

Data analysis

Statistical analyses were performed using MedCalc Statistical Software version 13.1.2 (MedCalc Software bvba, Ostend, Belgium). We first tested the effects of genotype by a one way ANOVA. To compare the effect of treatments (Opg-Fc, Dmab) and genotype (*HuRANKL-Tg+*, *Pparb*), we used a two way ANOVA. As appropriate, post hoc testing was performed using Fisher's protected Least Squares Difference (PLSD). Differences were considered significant at $p < 0.05$. Data are presented as mean ± SEM.

For humans analysis. To take into account that not all variables were normally distributed, the differences between groups were assessed by a Kruskal Wallis test, and spearman correlations between variables were analyzed.

References

1. Douni E, Alexiou M, & Kollias G (2004) Genetic engineering in the mouse: tuning TNF/TNFR expression. *Methods Mol Med* 98:137-170.
2. Nadra K, *et al.* (2006) Differentiation of trophoblast giant cells and their metabolic functions are dependent on peroxisome proliferator-activated receptor beta/delta. *Mol Cell Biol.* 26(8):3266-3281.
3. Fu H, Desvergne B, Ferrari S, & Bonnet N (2014) Impaired Musculoskeletal Response to Age and Exercise in PPARβ-/- Diabetic Mice. *Endocrinology* 155(12):4686-4696.
4. Picoli CC, *et al.* (2018) Peak Velocity as an Alternative Method for Training Prescription in Mice. *Front Physiol.* 9:42.
5. Chevalier C, *et al.* (2015) Gut Microbiota Orchestrates Energy Homeostasis during Cold. *Cell* 163(6):1360-1374.
6. Brun J, *et al.* (2017) Bone Regulates Browning and Energy Metabolism Through Mature Osteoblast/Osteocyte PPARγ Expression. *Diabetes* doi: 10.2337

7. Bouxsein ML, *et al.* (2005) beta-Arrestin2 regulates the differential response of cortical and trabecular bone to intermittent PTH in female mice. *J Bone Miner Res* 20(4):635-643.
8. Hildebrand T & Ruegsegger P (1997) A new method for the model-independent assessment of thickness in the three-dimensional images. *Journal of Microscopy* 185:67-75.
9. Bonnet N, *et al.* (2009) The matricellular protein Periostin is required for Sclerostin inhibition and the anabolic response to mechanical loading and physical activity. *J Biol Chem.* 284(51):35939-35950.
10. Kumar N & Dey CS (2003) Development of insulin resistance and reversal by thiazolidinediones in C2C12 skeletal muscle cells. *Biochem Pharmacol.* 65(2):249-257.
11. Bonnet N, Conway SJ, & Ferrari SL (2012) Regulation of beta catenin signaling and parathyroid hormone anabolic effects in bone by the matricellular protein periostin. *Proc Natl Acad Sci U S A.* 109(37):15048-15053.
12. Parfitt A. M, *et al.* (1987) Bone histomorphometry: standardization of nomenclature, symbols, and units. Report of the ASBMR Histomorphometry Nomenclature Committee. *J Bone Miner Res* 2(6):595-610.
13. Ribarič S & Čebašek V (2013) Simultaneous visualization of myosin heavy chain isoforms in single muscle sections. *Cells Tissues Organs.* 197(4):312-321.
14. Bonnet N, *et al.* (2017) Serum Levels of a Cathepsin-K Generated Periostin Fragment Predict Incident Low-Trauma Fractures in Postmenopausal Women Independently of BMD and FRAX. *J Bone Miner Res.* doi: 10.1002(jbmr.3203).
15. Biver E, *et al.* (2015) Prior ankle fractures in postmenopausal women are associated with low areal bone mineral density and bone microstructure alterations. *Osteoporos Int.* 26(8):2147-2155.
16. Chevalley T, Bonjour JP, van Rietbergen B, Ferrari S, & Rizzoli R (2013) Fracture history of healthy premenopausal women is associated with a reduction of cortical microstructural components at the distal radius. *Bone* 55(2):377-383.
17. Massera D, *et al.* (2018) Biochemical Markers of Bone Turnover and Risk of Incident Diabetes in Older Women: The Cardiovascular Health Study. *Diabetes Care* doi: 10.2337.
18. Durosier C, *et al.* (2013) Association of circulating sclerostin with bone mineral mass, microstructure, and turnover biochemical markers in healthy elderly men and women. *J Clin Endocrinol Metab.* 98(9):3873-3883.

Supplemental figures and figure legends

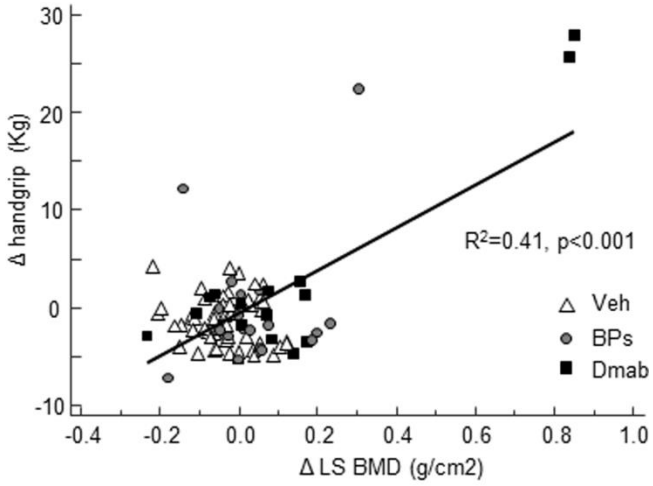

Fig. S1

Supplemental figure 1. Lumber spine BMD association with handgrip in GERICO cohort in control, bisphosphonate and denosumab patients.

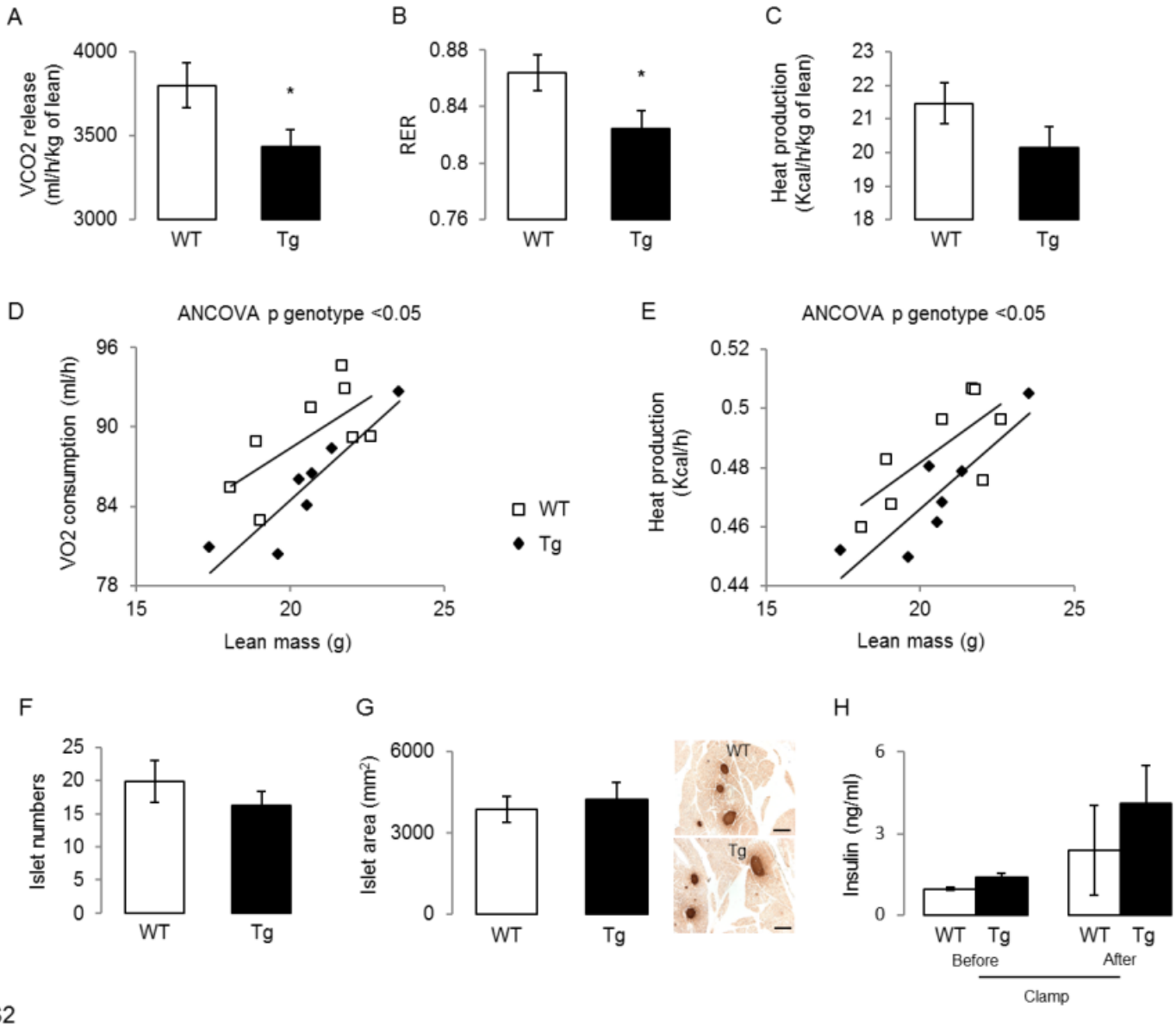

Fig. S2

Supplemental figure 2. Energy metabolism of adult huRANKLTg+. Energy metabolism was registered in metabolic cages during two consecutive days and nights (n = 6 per group). (A) CO2 releases (VCO_2). (B) Respiratory exchange ratio. (C) Heat production. (D-E) Plot between oxygen consumption and lean mass, and heat production and lean mass in WT and huRANKLTg+ mice. (F-G) Islet number and area calculate on peroxidase section of the insulin expression in the pancreas (n = 5 per group, bar = 150 µm). (H) Circulating levels of insulin before and after euglycemic-hyperinsulinemic clamp. * P<0.05 significant difference vs WT. Bars shows mean (± SEM). Closed bars, huRANKLTg+ ; open bars, *WT*.

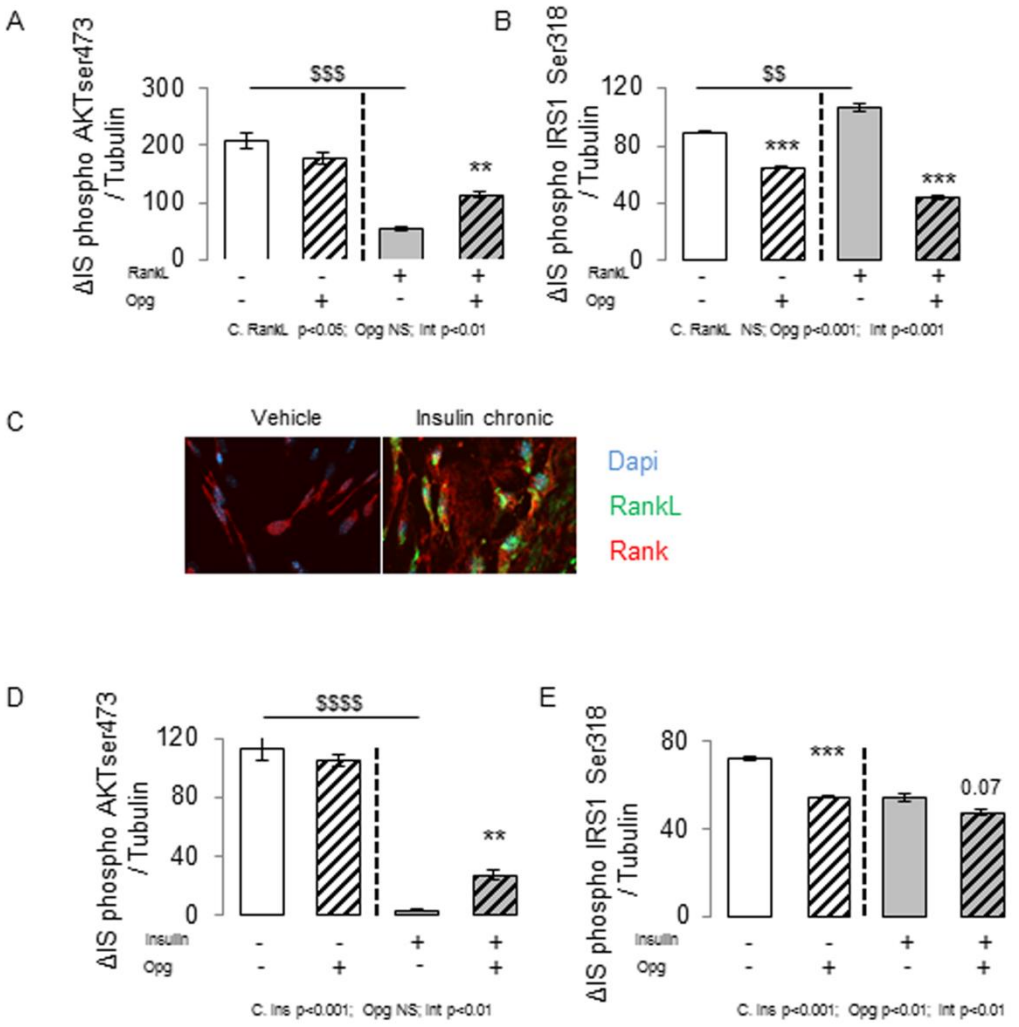

Fig. S3

Supplemental figure 3. OPG-Fc decreased insulin resistant and inflammation in C2C12 exposed to chronic RANKL or Insulin.

(A-B) Quantification of western figure 3C through Image J, histogram illustrates the amplitude response between Veh and insulin stimulation (ΔIS), * $P<0.05$, ** $P<0.01$ significant difference vs. No OPG respectively with chronic RANKL or not, $ $p<0.05$ significant difference vs. no RANKL-no OPG. (C) Immunohistochemistry of RANK, RANKL and Dapi in control and chronic insulin. (D-E) Histogram illustrates the amplitude response between Veh and insulin stimulation on western blot evaluated by image J (ΔIS), ** $P<0.01$, *** $P<0.001$ significant difference vs. Ctr respectively with chronic insulin or not, $$$$ $p<0.0001$ significant difference vs. no Insulin-no OPG.

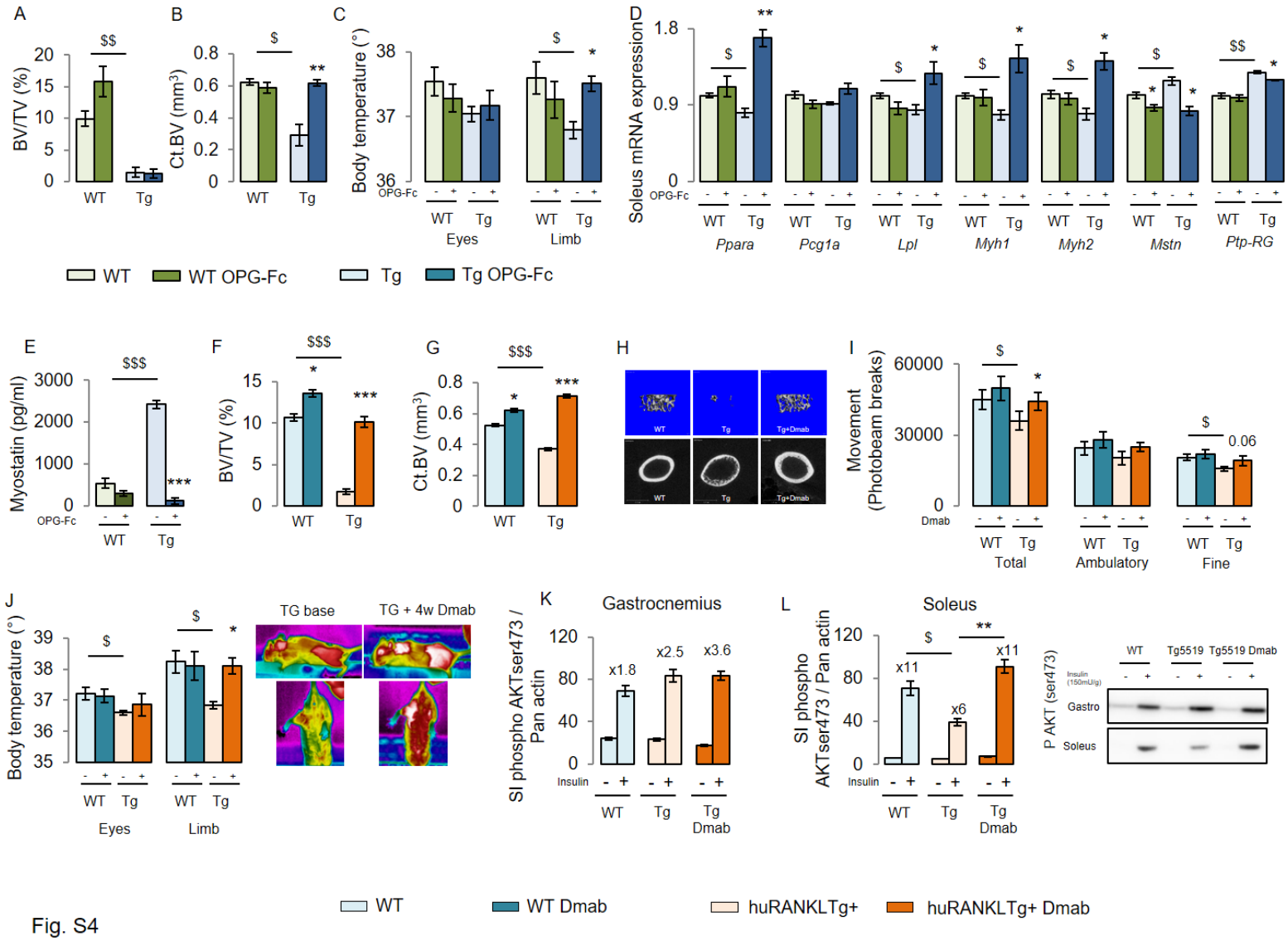

Fig. S4

Supplemental figure 4. Bone, muscle and insulin resistance of huRANKLTg+ treated by OPG-Fc and denosumab (Dmab). (A-B, E-F) Trabecular bone volume on tissue volume (BV/TV) at the distal femur and cortical bone volume (Ct.BV) at midshaft femur (*n* = 8 per group). (C,I) Body temperature evaluated by infrared camera, note the higher temperature of the limb of huRANKLTg+ after 4weeks of Dmab indicated by white spot (*n* = 8 per group). (D) Relative mRNA gene expression in soleus. (E) Circulating myostatin levels. (F-H) MicroCT images, upper panel: illustration of 3D trabecular structure of the distal femur, lower panel: illustration of 2D cortical structure of the midshaft femur. (I) Movement record in metabolic cages during two consecutive days and nights (*n* = 6 per group). (J) Body temperature. (K, L) Relative protein expression by western-blot in the gastrocnemius and soleus. * $P<0.05$, ** $P<0.01$, *** $P<0.001$ significant difference vs. saline. Bars show means (± SEM).

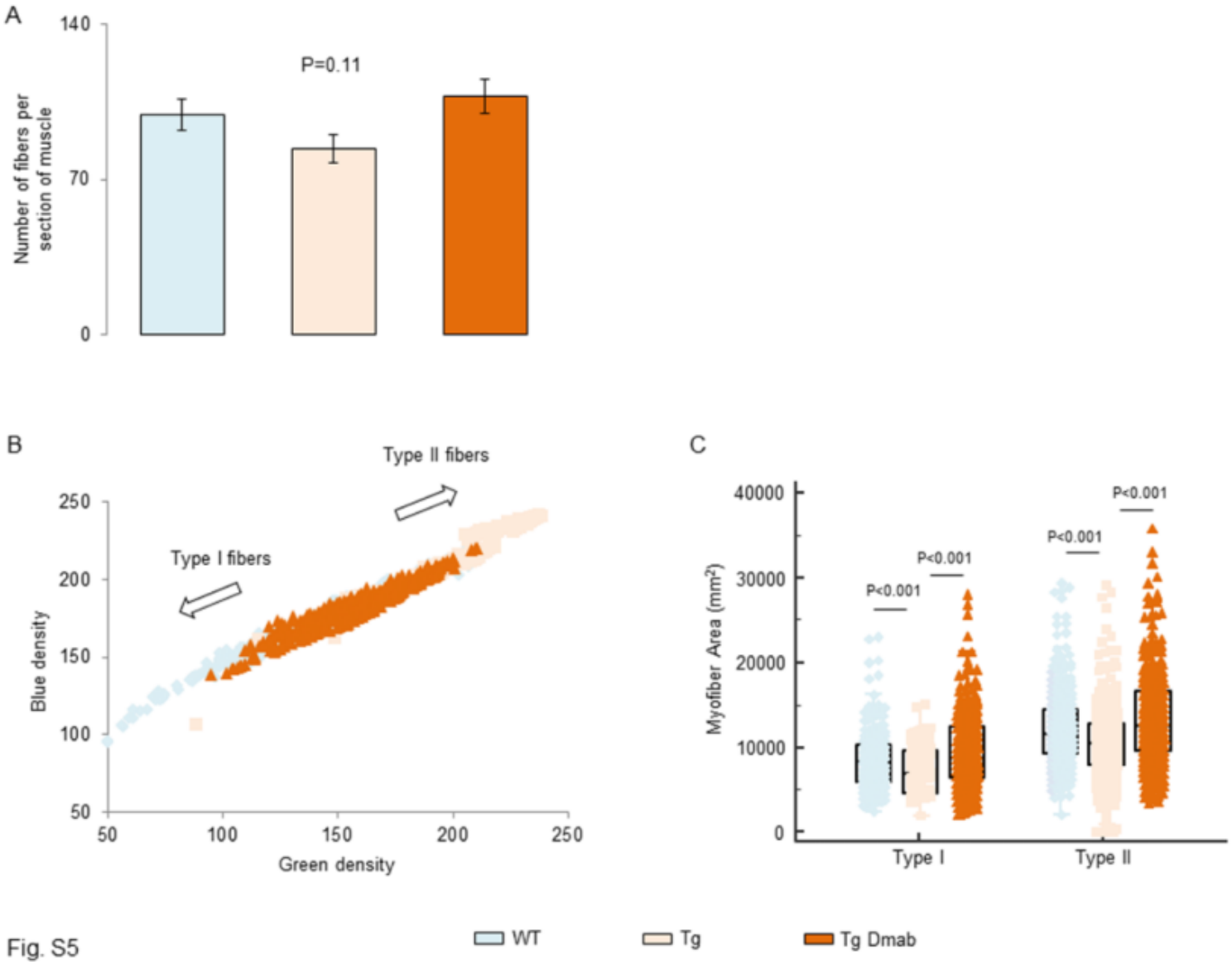

Fig. S5

Supplemental figure 5. Fibers type and area fibers of huRANKLTg+ treated by denosumab (Dmab). (A) Represent the distribution of type I and type II fibers between groups evaluated by blue levels intensity after succinate dehydrogenase staining. Intensity of the blue was automatically calculated using Bioquant Image Analysis Software. (B) Area of fibers per type of fibers I and II.

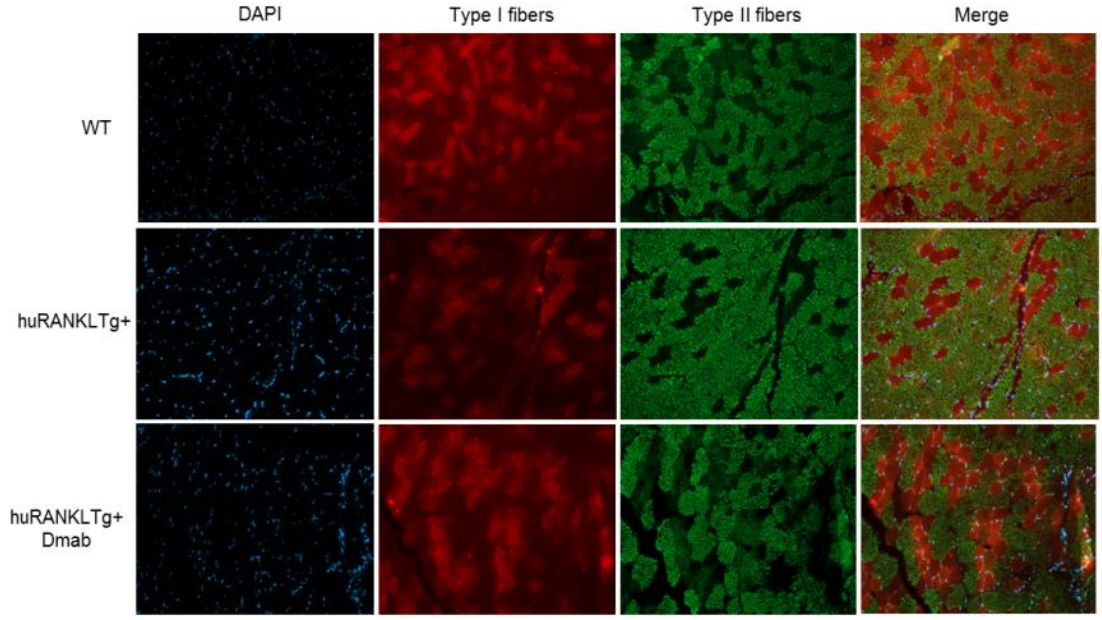

Supplemental figure 6. Fibers distribution in skeletal muscle of huRANKLTg+ treated by denosumab (Dmab). Immunohostchemistry were performed by using monoclonal antibodies BA-D5 for type I fibers (texas red) and SC-71 for type II (Alexi fluo 488, green).

Supplemental table 1. Clinical characteristics at baseline

	No-treatment (n=55)	BPs (n=20)	Dmab (n=18)	P value
Age (year)	65.0 ± 1.4	65.7 ± 0.9	64.9 ± 1.5	0.76
BMI (kg/m2)	23.9 ± 4.3	24.0 ± 4.6	24.2 ± 4.6	0.97
ALM (kg)	6.4 ± 0.9	6.7 ± 1.2	6.6 ± 1.1	0.51
Grip strength (kg)	26.6 ± 4.7	27.6 ± 5.4	26.9 ± 5.5	0.76
Fat mass (g)	22106 ± 8269	20794 ± 7768	23087 ± 7423	0.69
LS BMD (g/cm^2)	0.74 ± 0.11	0.70 ± 0.11	0.69 ± 0.10	0.14

BPs: Bisphosphonates (Alendronate n=8, Zoledronate n=12), ALM: Appendicular lean mass, LS: lumbar spine, BMD: Bone mineral density

Supplemental table 2. Influence of HuRANKL-Tg+ and Dmab on bone turnover markers.

	WT		HuRANKL-Tg+		p Geno	p Treat	p Int
	Vehicle	*Dmab*	*Vehicle*	*Dmab*			
Total Osteocalcin	86.4±9.2	25.6±3.3**	121.2±8.7$$	48.9±6.6***	**0.003**	0.001	**0.54**
Osteocalcin-Glu	3.7±0.3	1.6±0.1**	4.8±0.3$	2.3±0.2***	**0.003**	0.001	**0.66**
Myostatin	544±115	305±60**	2422±103$$$	120±73***	**0.001**	**0.001**	**0.001**

ELISA analysis performed at the femur after 4 weeks of Dmab or saline treatment. * $p<0.05$, ** $p<0.01$, ***$p<0.001$ vs vehicle (unpaired t test), p treatment, p genotype and p of interaction (p int). Fishers PLSD, 2F-ANOVA (n=8 mice / group). $ $p<0.05$, $$ $p<0.01$, $$$ $p<0.001$ vs WT. Means ± SEM.

Supplemental table 3. Influence of HuRANKL-Tg+ and Dmab on structure & remodelling indices at cortical and trabecular bone surfaces.

		WT		HuRANKL-Tg+		p Geno	p Treat	p Int
		Vehicle	*Dmab*	*Vehicle*	*Dmab*			
Endocortical	Ec MAR (µm/day)	1.49±0.14	1.55±0.13	6.86±1.03$$$	1.53±0.23***	**0.001**	**0.001**	**0.001**
	Ec sLPm (mm)	1.11±0.21	1.21±0.16	3.11±0.2$$$	2.41±0.26	**0.001**	0.21	0.10
	Ec dLPm (mm)	0.32±0.11	0.28±0.05	0.16±0.02$	0.60±0.20	0.71	0.14	0.14
	Ec BFR ($\mu m^2/\mu m$/ day)	1.40±0.32	1.37±0.19	11.88±2.24$$$	3.05±0.55**	**0.001**	**0.001**	**0.001**
Periosteal	Ps MAR (µm/day)	1.08±0.26	0.59±0.28	3.98±0.10$$$	0.24±0.19***	**0.001**	**0.001**	**0.001**
	Ps sLPm (mm)	1.26±0.24	1.45±0.39	1.80±0.47	0.57±0.23*	0.49	0.16	**0.02**
	Ps dLPm (mm)	0.94±0.37	0.24±0.11	4.61±0.33$$$	0.03±0.03***	**0.001**	**0.001**	**0.001**
	Ps BFR ($\mu m^2/\mu m$/ day)	2.13±0.75	0.79±0.36	22.02±2.75$$$	0.16±0.16***	**0.001**	**0.001**	**0.001**
Trabecular & cortical	BV/TV (%)	10.7±1.06	13.7±2.12	1.7±0.4$$$	7.7±1.5***	**0.001**	**0.001**	0.22
structure	Tb.N (1/mm)	4.5±0.2	4.3±0.3	1.5±0.1$$$	2.0±0.3*	**0.001**	0.16	0.51
	TbTh (um)	45.6±0.7	50.0±1.0**	51.8±0.4$$$	82.3±0.6***	**0.001**	**0.001**	**0.003**
	CtTV (mm^3)	1.12±0.05	1.36±0.05**	1.52±0.07$$$	1.98±0.16**	**0.001**	**0.001**	0.24
	CtBV (mm^3)	0.53±0.02	0.62±0.02**	0.39±0.02	0.71±0.06***	0.52	**0.001**	**0.002**
	CtTh (um)	199±3	194±7	97±4$$$	181±7***	**0.001**	**0.001**	**0.001**

Histomorphometric analysis performed at the femur after 4 weeks of Dmab or saline treatment. * p<0.05, ** p<0.01, ***p<0.001 vs vehicle (unpaired t test), p treatment, p genotype and p of interaction (p int). Fishers PLSD, 2F-ANOVA (n=8 mice / group). $ p<0.05, $$ p<0.01, $$$ p<0.001 vs WT. Means ± SEM Ps: periosteum, Ec: endocortical, Tb: trabecular. mineral apposition rate (MAR), Bone formation rate (BFR), single labelled perimeter (sLPm), double labelled perimeter (dLPm).

Supplemental table 4. Influence of Opg-Fc on structure & remodelling indices at cortical and trabecular bone surfaces of Pparβ$^{-/-}$ mice.

		WT	*Pparβ$^{-/-}$*	*Pparβ$^{-/-}$ Opg-Fc*	P grpe
Endocortical	Ec MAR (µm/day)	2.7±2.1	1.5±2.4	0.2±0.5	0.10
	Ec sLPm (mm)	2.8±1.6	2.0±0.7	0.4±0.5**	**0.002**
	Ec dLPm (mm)	0.43±0.37	0.36±0.56	0.01±0.03	0.16
	Ec BFR (µm^2/µm/ day)	4.70±4.6	3.12±4.84	0.02±0.04	0.12
Periosteal	Ps MAR (µm/day)	1.52±1.06	0.39±0.95	1.76±3.13	0.51
	Ps sLPm (mm)	3.87±2.6	4.26±1.86	3.03±2.03	0.57
	Ps dLPm (mm)	1.55±1.55	0.52±1.28	0.69±1.08	0.44
	Ps BFR (µm^2/µm/ day)	7.3±6.1	2.0±4.9	5.1±8.05	0.5
Trabecular & cortical	BV/TV (%)	5.8±1.2	3.9±2.0	7.8±2.7*	**0.05**
structure	Tb.N (1/mm)	3.0±0.4	2.1±0.3$	3.1±0.4*	**0.007**
	TbTh (um)	46.6±5	47.7±4**	52.0±7	**0.35**
	CtTV (mm^3)	0.43±0.03	0.52±0.04$	0.50±0.01	**0.001**
	CtBV (mm^3)	0.64±0.02	0.62±0.06	0.59±0.05*	0.24
	CtTh (um)	230±2	193±2$	210±1*	**0.004**

Histomorphometric analysis performed at the femur after 4 weeks of Opg-Fc or saline treatment. * p<0.05, ** p<0.01, ***p<0.001 vs vehicle (unpaired t test), p treatment, p genotype and p of interaction (p int). Fishers PLSD, 2F-ANOVA (n=8 mice / group). $ p<0.05, $$ p<0.01, $$$ p<0.001 vs WT. Means ± SEM Ps: periosteum, Ec: endocortical, Tb: trabecular. mineral apposition rate (MAR), Bone formation rate (BFR), single labelled perimeter (sLPm), double labelled perimeter (dLPm).